

# On tides in the ECMWF model

P.A.E.M. Janssen

Research Department

December 1999

This paper has not been published and should be regarded as an Internal Report from ECMWF.  
Permission to quote from it should be obtained from the ECMWF.



# On tides in the ECMWF model

---

**Peter A.E.M. Janssen**

European Centre for Medium-Range Weather Forecasts, UK

## Abstract

The theory of atmospheric tides has provided an explanation for the occurrence of short-period fluctuations in the tropical and sub-tropical surface pressure observations. These diurnal and semi-diurnal oscillations are, in principle, caused by the thermal forcing provided by the absorption of sunlight by stratospheric ozone and by water vapour. Here, we concentrate on the semi-diurnal oscillation which is called the  $S_2$  tide.

This study was started because in the ECMWF model it was found that the surface pressure amplitude of the  $S_2$  tide showed no sensitive dependence on the location of the top  $z_T$  of the model atmosphere. This follows from a comparison of the  $S_2$  tide from the 31 layer ( $z_T = 35$  km) and the recently introduced 50 layer ( $z_T = 70$  km) version of the ECMWF model. This insensitive dependence came as a surprise because the maximum of the ozone forcing in the Tropics is at about 50 km height, which is well above the top of the L31 model and well below the top of the L50 model. Returning to tidal theory, an explanation for the insensitive dependence of  $S_2$  surface pressure amplitude to the location of the top of the model atmosphere will be presented. It is related to the occurrence of spurious resonances in a bounded atmosphere resulting in a too large response to forcings. However, a relatively small increase of stratospheric temperature moves the relevant atmospheric oscillation closer to resonance with the forcing, resulting in a doubling of the tidal amplitude when the top of the atmosphere is moved from 35 to 70 km.

## 1. Introduction

The explanation of the amplitude and phase of the diurnal and semi-diurnal fluctuations seen in tropical and sub-tropical surface pressure observations has been debated for several centuries. Because the principal forcing was thought to be solar, the major component of the forcing was expected to have a period of one day and it was therefore surprising that at the surface the diurnal tide had a smaller amplitude than the semi-diurnal tide. In addition, the semi-diurnal tide showed a much more regular geographical pattern than the diurnal one.

Most of the historical account that follows is from *Chapman and Lindzen (1970)*. Kelvin and Raleigh suggested that the explanation for the apparent paradox was most likely in a near coincidence between the natural period of one of the atmospheric oscillations and 12 hours while such a close match would not occur for forcings on a diurnal time scale. To achieve the required amplification, one would need a nearly perfect resonance, so the difference between the natural periods and the semi-diurnal forcing should only be a few minutes at the most. In fact, a resting atmosphere almost has a natural resonance of 12.5 hours. Therefore, resonance seems not a very likely explanation for the occurrence of the  $S_2$  tide.

The period of the atmospheric oscillations depends in a sensitive manner on the vertical temperature profile  $T(z)$ . *Jacchia and Kopal (1951)* proposed a temperature profile which would yield the greatest amplification factor for the semi-diurnal oscillation. However, rocket measurements of  $T(z)$  did not agree with the tentative Jacchia-Kopal profile which gave too high a temperature (320 K to 350 K) at the stratopause at about 50-60 km height. The rocket results definitely excluded the possibility of a considerable magnification of the  $S_2$  tide by resonance and thus undermined Kelvin's hypothesis.

An alternative explanation of the  $S_2$  tide was therefore needed and one was suggested by *Siebert (1954)* and by *Sen and White (1955)*. Before that time, the thermal excitation of  $S_2$  was thought to come from temperature fluctuations caused by the upward eddy conduction from the ground. The ground was tacitly supposed to be the only absorber of the solar radiation. However, some of the radiation is absorbed during its passage through

the air. *Siebert* (1961) estimated that absorption by water vapour may explain 30% of the amplitude of the  $S_2$  tide while *Butler and Small* (1963) found that ozone heating could account for about two thirds of the observed amplitude of the  $S_2$  tide. Therefore, the combination of water vapour and ozone absorption explains the occurrence of the  $S_2$  tide to a large extent. The present day explanation of the  $S_2$  tide therefore does not rely on resonance and thus there is no theoretical need for a highly tuned atmosphere.

The diurnal tide is excited for the same reason, but there is an important difference in the vertical structure of the  $S_1$  and  $S_2$  tide. Regarding  $S_2$ , the forcing projects mainly on a single free mode of the atmosphere while for  $S_1$  the forcing projects on a number of modes which are either trapped in the vertical or which propagate vertically with a fairly short wavelength and tend to interfere. As a consequence, near the surface the semi-diurnal tide will dominate the diurnal tide, in particular in the surface pressure in the Tropics. The semi-diurnal wave migrates westward following the sun and has zonal wave number two. Its geographical pattern is therefore very regular. The diurnal component of the pressure oscillation, increases with height and dominates the semi-diurnal signal in the upper troposphere. Because it has low amplitude near the surface, the diurnal signal is complicated by local effects related to land/sea contrasts, diurnally varying heating of land by solar radiation and orographically-induced oscillations. Its geographical structure is therefore less regular as it consists of both a propagating wave with wave number 1 and standing wave components forced by the major continents.

Several studies investigated how well atmospheric models represent the  $S_1$  and  $S_2$  components of the atmospheric tide. *Zwiers and Hamilton* (1986) studied tides in a version of the Canadian climate model, while *Hsu and Hoskins* (1989) studied the performance of a version of the ECMWF model. We will concentrate, because of its simplicity, on the  $S_2$  tide.

The quality of the model results was judged against an empirical description of *Haurwitz* (1956) who found that the amplitude and phase of the travelling wave component of the semi-diurnal surface pressure oscillation is given by

$$\delta p = 1.16 \cos^3(\phi) \sin(2t + 158^\circ) \text{mb}$$

where  $\phi$  is latitude and  $t$  is local time (normalised with the length of day times  $2\pi$ ). The fit was obtained from long time series of surface pressure data from 296 stations.

Both models gave accurate results regarding the phase of the  $S_2$  tide. The Canadian model underestimated the tidal amplitude while the ECMWF model appeared to be in closer agreement with the empirical description of *Haurwitz*.

Many atmospheric models have a lid at the top of the model atmosphere around a pressure level of 10 mb which corresponds to a height of 30 km. Therefore, an important part of the forcing of solar radiation absorption by ozone (which has its maximum at around 50 km height) is not taken into account by these atmospheric models. One would therefore expect a considerable underestimation of the  $S_2$  atmospheric tide by the models, but surprisingly in the above models this does not occur. An explanation for this was provided by *Lindzen et al* (1968) who found that the lid gives rise to spurious resonances resulting in a too large response to forcing. *Zwiers and Hamilton* (1986) reinvestigated this question in the context of a simple tidal theory and they found hardly any dependence of tidal amplitude on the location of the top of the atmosphere.

*Hsu and Hoskins* (1989) pointed out, however, that such a tidal theory is too simple to represent reality in a viable way, leaving open the question of the dependence of tidal amplitude on the height of the atmosphere and on the formulation of the boundary condition at the top of the atmosphere.

ECMWF recently moved the top of the model atmosphere by a factor of two to 65 km, therefore the ozone contribution to the forcing of the  $S_2$  tide is now well-represented by the model. Remarkably, there are only minor differences between the  $S_2$  tide of the old version of the atmospheric model (which had 31 layers) and the present 50 layer operational model. This is clearly shown in Fig 1 where the spatial distribution of the day 1 forecast  $S_2$  tide from the 31 layer and 50 layer is compared. Each plot is obtained by taking a monthly average (in this case of the month of January) of the 12,18,24 and 30 hour forecast of surface pressure and the  $S_2$  tide at 12 GMT follows from  $(24+12-(18+30))/4$ .

Thus, the insensitive dependence of the  $S_2$  tidal amplitude on the thickness of the atmosphere is also found in simulations by means of the ECMWF model. Nevertheless, I did not feel very comfortable with this result so I decided to revisit this issue in the context of a simple tidal theory. For certain choices of the vertical temperature profile indeed the amplitude of the  $S_2$  tide is quite insensitive to the thickness of the atmosphere. However, this conclusion depends in a sensitive way on how the temperature profile is modelled in the stratosphere and, by increasing the temperature around 50 km by a relatively small amount, a sensitive dependence of the  $S_2$  amplitude as function of the height of the atmosphere may be obtained. The reason for this is that the free atmospheric modes move closer to the resonance with the forcing of solar radiation by ozone.

The programme of this paper is as follows. In Section 2 we briefly present the well-known model for the  $S_2$  tide as already discussed by Chapman and Lindzen. In order to obtain the amplitude of the surface pressure oscillation, one needs to solve an inhomogeneous second order differential equation for the vertical structure function where the source function represents the effect of absorption of solar radiation by ozone and water vapour. In Section 3 a gaussian elimination method is used to solve the differential equation for the vertical structure function. The differential equation has a number of turning points in such a way that waves are vertically propagating in the stratosphere, while they are trapped near the surface and above 60 km. Because of the delicate behaviour of the solution near the turning points the results from the gaussian elimination method are compared with a perturbation approach based on small wave number in the vertical. The agreement is satisfactory, while in lowest order the perturbation approach reveals how the surface pressure amplitude depends on details of the forcing by water vapour and ozone.

In Section 4 it is shown that for a temperature profile that resembles that of the ECMWF model the surface pressure amplitude of the  $S_2$  tide is indeed insensitive to a change in the thickness of the atmosphere by a factor of two. The ECMWF model temperature is at 50 km height too low by 15K and, by increasing the temperature in the 'lower' stratosphere resonance between the forcing and the tidal oscillations becomes relevant and a much more sensitive dependence of the  $S_2$  tidal amplitude on the thickness of the atmosphere is found. Our conclusions are presented in Section 5 while, in the Appendix, it is pointed out that the study of the  $S_1$  and  $S_2$  tide in the model atmosphere may be useful in analysing changes in the analysis and forecasting system. As an example, we discuss the introduction of the new  $J_B$  in 3DVAR which had a considerable impact on the analysed  $S_1$  and  $S_2$  tide.

## 2. Tidal theory

Let us study the problem of the excitation of the  $S_2$  tide in somewhat more detail, where the starting point is the treatment of tides as given by *Chapman and Lindzen (1970)* (where also an extensive discussion on the assumptions involved is given).

Basically, one linearizes the relevant equations around the basic state given by the density distribution  $\rho_o(z)$  with height  $z$  and pressure distribution  $p_o(z)$  and one seeks separable solutions of the type

$$f = g(\theta, z) \exp i(\sigma t + s\phi) \quad (1)$$

where

$$g(\theta, z) = \Theta(\theta)y(z) \quad (2)$$

and  $\theta$  is latitude,  $\phi$  is longitude,  $\sigma$  is the oscillation frequency and  $s$  is a mode number which can have the values  $0, \pm 1, \pm 2, \dots$

In terms of the variable

$$G = -\frac{1}{\delta\gamma p_o} \frac{D}{Dt} P \quad (3)$$

where  $\gamma = c_p/c_v = 1.4$  the resulting partial differential equation in  $\Theta$  and  $z$  assumes a relatively simple form. It may be solved by the method of separation of variables. To that end one writes

$$G^{\sigma, s} = \sum_n L_n^{\sigma, s}(z) \Theta_n^{\sigma, s}(\theta) \quad (4)$$

where the set  $\Theta_n^{\sigma, s}$  is assumed to be complete, and similarly the forcing by absorption of solar radiation, denoted by  $J$ , is expanded in a similar fashion

$$J^{\sigma, s} = \sum_n J_n^{\sigma, s}(z) \Theta_n^{\sigma, s}(\theta) \quad (5)$$

As a result one arrives on the one hand at Laplace's tidal equation (with Hough functions as its solution), while on the other hand one finds the vertical structure equation

$$\frac{d^2}{dx^2} y_n + k_n^2(x) y_n = \frac{i\sigma R}{\gamma g h_n} \tau_n e^{-x/2} \quad (6)$$

where

$$k_n^2(x) = \frac{1}{h_n} \left( \kappa H + \frac{dH}{dx} \right) - \frac{1}{4} \quad (7)$$

$H$  is the scale height  $RT_o/g$ ,  $\kappa = (\gamma-1)/\gamma$ ,  $T_o$  the temperature profile,  $g$  acceleration of gravity,  $x = -\log(p_o(z)p_o(o))$  and  $y_n = e^{-x/2} L_n$ .

The separation constant  $h_n$  follows from the solutions of Laplace's equation. For the  $S_2$  tide with  $s=2$  one finds  $h_n \cong 7.852$  km.

Furthermore, the right-hand side of Eq (5) represents the forcing function of the atmospheric waves; the forcing functions  $\tau_n = \kappa J^{s,s} h_n \sigma R$  for  $H_2O$  and  $O_3$ , obtained from *Chapman and Lindzen (1970)*, are given in Fig 2. The shape of the latitude dependence for the diurnal and semi-diurnal excitations is very similar, however, as is evident from Fig 2, the amplitude of the diurnal excitation is much larger than the semi-diurnal one. Regarding the phase, it is noted that the diurnal excitation has maximum amplitude at 1800 LT while the semi-diurnal excitation has a maximum at 0300 and 1500 LT.

The  $S_2$  tidal problem now derives its simplicity from the fact that the latitude distribution of the forcing is very similar to the shape of one of the relevant semi-diurnal Hough modes, while for the  $S_1$  problem a mixture of Hough modes is involved. As already mentioned, the dominant semi-diurnal Hough mode has an equivalent depth of about 7.8 km and for realistic temperature profiles the wave number  $k_n$  is quite small corresponding to extremely long vertical wave lengths of ca. 150 km. Thus, not only does this Hough mode receive the bulk of the semi diurnal excitation, but it responds to this excitation with high efficiency - the main excitation corresponds in 'phase'!!

Providing the vertical structure equation (5) with boundary conditions one can solve for  $y_n$  and the pressure perturbation and the vertical velocity follow from

$$\begin{aligned} \delta p_n &= \frac{p_o(o) \gamma h_n}{H(x) i \sigma} e^{-x/2} \left( \frac{d}{dx} y_n - \frac{1}{2} y_n \right) \\ \delta w_n &= \gamma h_n e^{-x/2} \left[ \frac{d}{dx} y_n + \left( \frac{H}{h_n} - \frac{1}{2} \right) y_n \right] \end{aligned} \quad (8)$$

The lower boundary condition is simply that there is no vertical motion at the surface, hence

$$x = 0: \frac{d}{dx} y_n + \left( \frac{H}{h_n} - \frac{1}{2} \right) y_n = 0 \quad (9)$$

For the upper boundary condition one usually takes the radiation condition that only waves propagating upwards are allowed, which assumes that there are no sources at infinity. However, the ECMWF model has a rigid lid on top of the atmosphere, thus at  $x = x_T$   $\delta w$  vanishes as well:

$$x = x_T: \frac{d}{dx} y_n + \left( \frac{H}{h_n} - \frac{1}{2} \right) y_n = 0 \quad (10)$$

Therefore, in order to obtain the surface pressure amplitude from (6), one has to solve the inhomogeneous differential equation (5) subject to the boundary conditions (7) and (8) but, of course, the wave number  $k_n$  (and hence the vertical temperature profile) needs to be given. Initial attempts at solving the problem gave noisy results because a discretization of the equatorial temperature profile of *Chapman and Lindzen (1970)* was used. Smoother results were obtained with the following analytical temperature profile

$$T_o(z) = 240 - Bz + A \exp(\alpha z) \cos(l(z)z) \quad (11)$$

with  $l(z) = l_o \exp(\beta z)$ ,  $A = 60$ ,  $\beta = -1/400000$  and  $l_o = \pi/23000$ . Results will be presented for two choices of temperature profiles, namely one that resembles the ECMWF mean profile (with  $\alpha = -1/100000$  and  $\beta = 0.0003$ ) and one that resembles Chapman and Lindzen's equatorial profile ( $\alpha = -1/400000$  and  $\beta = 0.00003$ ). They are displayed in Fig 3 while Fig 4 shows  $k_n^2(z)$  as function of height. For the chosen temperature profiles it is seen that between  $z=22$  and  $55$  km the atmospheric waves are propagating while in the troposphere and above  $55$  km they are trapped. Depending on the choice of temperature profile there are 3 to 4 turning points where  $k_n^2$  vanishes.

Finally, the forcing functions for  $O_3$  and  $H_2O$  need to be specified. We calculate the tidal amplitude on the equator only, while the vertical distribution of the forcing is parametrized by

$$\tau_{H_2O} = \tau_m^v \exp(-\beta_v z)$$

and

$$\tau_{O_3} = \tau_m^{o_3} \exp\left(-\frac{1}{2} \left(\frac{z - z_m}{\sigma_{O_3}}\right)^2\right) \quad (12)$$

where, in agreement with Fig 2, we take  $\tau_m^v = 0.035$ ,  $\beta_v = 0.3/H_{Ref}$ ,  $\tau_m^{o_3} = 0.32$ ,  $z_m = 6.8H_{Ref}$  and  $\sigma_{O_3} = 2H_{Ref}$  where the reference scale height  $H_{Ref} = 7600$  m. It is noted that the forcing functions are still to be multiplied by the function  $\exp(-x/2)$  so that, as may be inferred from Fig 5, the forcing by  $O_3$  and  $H_2O$  is of equal importance. Nevertheless,  $O_3$  is providing the dominant excitation contribution to the  $S_2$  tide, because this excitation occurs just in that part of the atmosphere where the free waves propagate in the vertical, while the water vapour excitation occurs in that part of the atmosphere where the waves are damped in the vertical.

In the experiments with varying thickness of the atmosphere we add to the ozone forcing in the top layer the total forcing contribution coming from the part of the atmosphere which is above the top layer. This mimics the ECMWF practice regarding the ozone concentration.

### 3. Solution of the boundary value problem

We describe an efficient numerical scheme, due to *Bruce et al (1953)* and we comment on its application to the boundary value problem given in Section 2. To that end divide the  $x$ -domain into a number of discrete

levels  $x_0, x_1, \dots$  where  $x_0 = 0$  and the remaining levels are equally spaced with separation  $\Delta x$ . At  $x_m$  the derivatives of  $y$  are approximated as

$$\begin{aligned}\frac{d}{dx}y &= \frac{y_{m+1} - y_{m-1}}{2\Delta x} \\ \frac{d^2}{dx^2}y &= \frac{y_{m+1} - 2y_m + y_{m-1}}{(\Delta x)^2}\end{aligned}\quad (13)$$

Here the subscripts refer to the level where  $y$  is evaluated and the subscript  $n$  of the previous section has been dropped. Using (11) the differential equation (5) may be written as

$$A_m y_{m+1} + B_m y_m + C_m y_{m-1} = D_m \quad (14)$$

where

$$\begin{aligned}A_m &= C_m = 1 \\ B_m &= -2 + \Delta x^2 k^2(x_m) \\ D_m &= \Delta x^2 \frac{i\sigma R}{\gamma g h_n} \tau(x_m) e^{-x_m/2}\end{aligned}$$

Chapman and Lindzen solved the system (12) by posing

$$y_m = \alpha_m y_{m+1} + \beta_m$$

where  $\alpha_m$  and  $\beta_m$  follow from (14), thus the system of equations is solved from top to bottom. It turned out, however, that  $\alpha_m$  and  $\beta_m$  showed singular behaviour for  $m$  corresponding to  $x \approx 4$ , and therefore we tried to solve (14) from bottom to top, i.e.

$$y_m = \alpha_m y_{m-1} + \beta_m \quad (15)$$

which did not show singular behaviour, but nevertheless gave identical results. Substituting (15) into (14) gives

$$\alpha_m = \frac{C_m}{A_m \alpha_{m+1} + B_m}, \quad \beta_m = \frac{D_m - A_m \beta_{m+1}}{A_m \alpha_{m+1} + B_m} \quad (16)$$

Let  $m = M$  correspond to the top level. The values of  $\alpha_M$  and  $\beta_M$  then follow from the boundary condition at the top of the atmosphere, Eq (10). Discretizing the derivative at the top as  $\frac{dy}{dx} \equiv (y_M - y_{M-1})/\Delta x$  one finds that

$$y_M - y_{M-1} = -\delta y_M \Delta x$$

with  $\delta(x_T) = H(x_T)/h_n - \frac{1}{2}$ . Using (15) to eliminate  $y_{M-1}$  one obtains



$$\alpha_M = \frac{1}{1 + \delta \Delta x}, \quad \beta_M = 0 \quad (17)$$

and therefore  $\alpha_m$  and  $\beta_m$  may be obtained at once for  $m < M$ .

In order to solve (15) one finally needs the value of  $y_o$ , which follows from the boundary condition (7) at the bottom of the atmosphere. One then finds

$$y_o = -\beta_1 / (\alpha_1 - 1 + \delta(0)\Delta x) \quad (18)$$

This integration scheme is particularly efficient because only one pass is needed to solve the two-point boundary value (6, 9, 10), which contrasts with the usual shooting technique one usually employs to solve this kind of problem.

According to *Chapman and Lindzen* (1970) this numerical method works for slowly varying vertical wave number  $k_n(x)$ . However, referring to Fig 4, it is evident that because of the presence of turning points in  $k_n^2$  the condition of slowly varying  $k_n(x)$  is not guaranteed. It was therefore thought worthwhile to compare results of the present scheme with alternative, semi-analytical approaches.

An obvious approach would be to apply the JWKB technique which involves a turning point analysis in terms of Airy functions. Thus, at every turning point  $k_n^2$  is approximated by a linear function of the distance from the turning point (times the derivative of  $k_n^2$ ). Hence, near this point the solution is a linear combination of two linearly independent Airy functions and usually the solution can be continued to the next turning point by asymptotic matching. For the problem at hand, however, the turning points are so close together that asymptotic matching fails. In other words,  $k_n^2$  is not a slowly varying function of height (cf Fig 4) and the JWKB technique may therefore not be applied in this case.

An alternative semi-analytical approach is to assume small wave number  $k_n$  and to obtain a series solution by iteration. The Eqns (6, 9, 10) are therefore written as

$$\begin{aligned} Ly - S &= -\varepsilon k^2 y \\ x = 0: dy/dx &= -\delta_o y \\ x = x_T: dy/dx &= -\delta_T y \end{aligned} \quad (19)$$

where  $L = d^2/dx^2$ ,  $S$  represents the forcing function by ozone and water vapour and  $\delta = H/h_n - \frac{1}{2}$ . The parameter  $\varepsilon$  is introduced to indicate that the wave number  $k$  is assumed to be small. Afterwards,  $\varepsilon = 1$  is taken.

We seek a solution for small  $k$ , therefore

$$y = \sum_{n=0}^{\infty} \varepsilon^n y_n \quad (20)$$

and in lowest order we find

$$\begin{aligned}
 Ly_o &= S(x) \\
 x = 0: dy_o/dx &= -\delta_o y_o \\
 x = x_T: dy_o/dx &= -\delta_T y_o
 \end{aligned}
 \tag{21}$$

The solution of the problem (19) is

$$y_o = \int dx' G(x, x') S(x')$$

where

$$\bar{G}(x, x') = \begin{cases} x' > x, (1 - \delta_o x) (1 + \delta_T(x_T - x'))/N \\ x' < x, (1 - \delta_o x')(1 + \delta_T(x_T - x))/N \end{cases}
 \tag{22}$$

with  $N = \delta_o + \delta_T(\delta_o x_T - 1)$ . Remark that the Green's function  $G$  should be symmetrical with respect to interchange of  $x$  and  $x'$ .

All higher order corrections obey the system

$$\begin{aligned}
 Ly_n &= -k^2 y_{n-1} \\
 \frac{dy_n}{dx} &= -\delta_o y_n \\
 \frac{dy_n}{dx} &= -\delta_T y_n
 \end{aligned}$$

and therefore

$$y_n = -\int dx' G(x, x') k^2(x') y_{n-1}(x') \tag{23}$$

where the Green's function is given by (22). The complete solution may therefore be obtained by successively solving (23) and the surface pressure amplitude follows from (8) at once.

We remark that the zeroth order solution for surface pressure may be cast in a relatively simple form if one takes the limit of large thickness of the atmosphere,  $x_T \rightarrow \infty$ . In that event, one finds from Eq (22) for  $x \rightarrow 0$ ,

$$y_o(o) = \frac{1}{\delta_o} \int_0^\infty dx S(x) \tag{24}$$

Use of Eq (8) then finally gives for the surface pressure amplitude

$$\frac{\delta p(0)}{p_o(0)} = -\frac{R}{gh_n \delta_o} \int_0^{\infty} dx \tau(x) e^{-x/2} \quad (25)$$

and hence in the limit of small wave number  $\delta p(o)$  is proportional to the integral of the total forcing, displayed in Fig 5. This elegant result may be further simplified by using the forcing functions given in Eq (12) for constant scaling height  $H$  in the limit of large  $x_m$  and small  $\sigma_o$ . The result is

$$\frac{\delta p(o)}{p_o(o)} = -\frac{R}{gh_n \delta_o} \left[ \frac{\tau_m^v}{\beta_v H + \frac{1}{2}} + \sigma \tau_m^{o_3} \sqrt{2\pi} e^{-\frac{1}{2} \left( \frac{z_m}{H} - \frac{1}{4} \sigma^2 \right)} \right] \quad (26)$$

where  $\sigma = \sigma_o/H$ . We remark that since  $x_m$  is large, the ozone contribution depends in a sensitive way on the precise location of the maximum of the ozone forcing. Eq (26) allows us to estimate the relative contributions from water vapour and ozone. Using the numbers from Eq (12) one finds that water vapour contributes 40% to the  $S_2$  tidal amplitude while ozone has a 60% contribution. Therefore, the 'major' contribution to the  $S_2$  tide is from the ozone forcing.

In general, the zero wave number solution will underestimate the tidal amplitude at the surface. We have illustrated this in Fig 6 where the surface pressure amplitude is plotted versus the thickness of the atmosphere for different iterations of the scheme (22)-(23). As temperature profile we took the ECMWF mean profile (cf Eq (11)). In addition, it is evident from Fig 6 that the iteration scheme converges fairly rapidly. To make sure of this the 10th order solution (not shown) gave almost identical results as the fifth order solution, thus providing confidence in the solution method.

We compare the results from the Gaussian elimination method with results of the iteration method in Fig 7, and a fair agreement is obtained. Thus we are confident in using the Gaussian elimination method despite the fact that the wave number  $k_n(x)$  is not slowly varying; we prefer this method because it is a very fast one.

Before closing this Section we comment on the phase of the tidal wave. As already noted in Section 2, the semi-diurnal excitation has a maximum at 3 o'clock in the morning and in the afternoon local time. Combined with the  $180^\circ$  phase shift in the pressure (see Eq (26)) which implies a shift of 6 hours, the result is that the pressure has a maximum at 9 o'clock in the morning and evening. This is at variance with the fit by Haurwitz which suggests a maximum close to 10 o'clock.

We remark that it is straightforward to show that simple tidal theory does not give a phase shift (apart from  $180^\circ$ ) when the rigid lid condition on top of the atmosphere is imposed. This follows from reality of the Green's function (22) and therefore to all orders Eq (23) will not produce a phase shift. A radiation condition at the top of the atmosphere might result in a phase shift (provided one deals with an outgoing wave and not a damped one). However, atmospheric models such as the one from ECMWF have a rigid lid condition and, in spite of this, these models produce a reasonable phase of the  $S_2$  tide (This follows immediately from Fig.1 which shows in the Tropical Atlantic a maximum at 30 deg. West which corresponds to a two hour phase shift). It may therefore be the case that simple tidal theory does not provide the complete explanation of the  $S_2$  tide, and that additional effects such as latent heat release (cf Hamilton, 1981) need to be introduced. But

to first order this theory seems to give an adequate explanation of the semi-diurnal tide and in the next section we apply it to the problem of the dependence of surface pressure amplitude on the thickness of the atmosphere.

#### 4. Results with emphasis on sensitive dependence on the temperature profile

In order to study the dependence of the tidal amplitude on the thickness of the model atmosphere, we applied the Gaussian elimination method with 300 layers in the vertical. The forcing functions were taken as in Eq (12) while we start with a temperature profile that resembles the ECMWF mean profile (cf below Eq (11)). The boundary condition at the top of the atmosphere is the rigid lid condition.

We did experiments with the radiation condition as well, although this condition is not relevant for the comparison with weather prediction models. Instead of Eq (10) one would take as condition

$$x = x_T: \frac{d}{dx} y_n = -ik_n(x_T)y_n \quad (27)$$

and one would get a sensitive dependence of tidal amplitude on  $x_T$ . The reason for this is that  $k_n(x)$  is a sensitive function of  $x$  and, depending on the location of  $x_T$  (cf Fig 4), one may impose the condition of an outgoing wave or the one for a damped wave. Also, strictly speaking one should only apply the radiation condition where the effect of forcing is small. This is clearly not the case for the smaller values of  $x_T$ .

One of our main results is shown in Fig 8, where we have plotted the surface amplitude of the  $S_2$  tide as function of the thickness of the atmosphere  $x_T$ . For reference we remark that the L31 ECMWF model which has its top at 10 mb corresponds to  $x_T=4.6$ , while the L50 model (with its top at 0.1 mb) corresponds to  $x_T=9.2$ . The black line corresponds to the case of forcing by ozone and water vapour and, in agreement with the model simulations of Fig 1, there is only a weak dependence of tidal amplitude on the thickness of the atmosphere. In an attempt to try to understand this weak dependency, we have also plotted the contributions by water vapour, ozone and ozone (only the resolved part) separately.

The tidal amplitude excited by absorption of radiation by water vapour only, decreases very slightly with increasing thickness of the atmosphere, though one would perhaps expect the reverse. This is presumably caused by the confinement of tidal energy in the model by the rigid lid and the consequent intensification of the response. A similar remark applies to the ozone response curve. But here the dependence of tidal amplitude on  $x_T$  is even weaker because of the addition of the unresolved part of the absorption by ozone in the top layer. This follows from a comparison of the curve labelled  $O_3$  and labelled  $O_3$  (resolved only).

We remark that we have performed our experiments with a fixed number of layers, rather than a fixed resolution in the vertical. If one would perform experiments with a fixed vertical resolution, then a further weakening of the  $x_T$  dependence of tidal amplitude will be found since it can be shown numerically (cf also *Zwiers and Hamilton, 1986*) that a higher resolution in the vertical will result in a smaller response.

It is concluded that for small thickness of the atmosphere  $x_T$  the confinement of tidal energy by the rigid lid compensates for the lack of forcing by ozone. Combined with the observation that for the ECMWF temperature profile ozone and water vapour are equally important (contrary to common belief) the result is a

weak dependence of tidal amplitude on  $x_T$ . This conclusion is more or less in agreement with the findings of *Zwiers and Hamilton* (1986).

Further study of the problem revealed, however, that this conclusion depends in a sensitive way on the choice of the temperature profile. In the stratosphere around 50 km height it is known that the 50 layer ECMWF model underestimates temperature by perhaps as much as 15° K. From the history of the problem (cf the Introduction) it is known that the temperature profile in the stratosphere controls, to a large extent, the near-resonance between the forcing and the relevant free mode of the atmosphere. By using the Chapman and Lindzen equatorial mean temperature profile, instead of the ECMWF one, a somewhat different picture emerges, as shown in Fig 9. There is now a sensitive dependence of tidal amplitude on  $x_T$ , while for large  $x_T$  ozone is providing the major excitation mechanism for the  $S_2$  tide. It is emphasised that this sensitive dependence follows because, by increasing the temperature maximum in the stratosphere, the system moves closer towards resonance.

## 5. Conclusions

We have made an attempt to explain the insensitive dependence of the  $S_2$  surface pressure amplitude on the thickness of the atmosphere. For a class of temperature profiles which have a relatively low stratospheric maximum we also find this insensitive dependence when applying the classical tidal theory. An increase of the maximum temperature by some 20K gives, however, a more sensitive dependence of tidal amplitude.

Therefore we have the impression that this weak dependence of tidal amplitude, as seen in simulations with the ECMWF model, is a lucky coincidence because the stratospheric temperature maximum is too low while an increase of this maximum will probably result in a more sensitive response to forcing by ozone. A relatively small increase of stratospheric temperature moves the relevant free atmospheric wave closer to resonance with the forcing, resulting in doubling the tidal amplitude. Although resonance was rightly discarded as providing the only explanation for the occurrence of the semi-diurnal oscillation, we have nevertheless shown that resonance is still relevant for the tidal problem in models.

In the Appendix we discuss the usefulness of tidal maps in studying systematic errors in atmospheric models. Based on a comparison of first-guess and analysed  $S_1$  and  $S_2$  tides, combined with the empirical evidence of Haurwitz, it is concluded that modelled tidal amplitudes are too large whilst in the tropical Atlantic the first-guess  $S_2$  maximum is reached too early by almost an hour.

In conclusion, we remark that it may be worthwhile to study in more detail the forcing mechanism of the diurnal and semi-diurnal tide in the ECMWF model. At this point removal of the cold temperature bias, which will drive the atmospheric system closer to resonance, will make things even worse because even larger tidal amplitudes are expected.

## Acknowledgement

Useful discussions with Tony Hollingsworth, Adrian Simmons, Jean-Jacques Morcrette, Clive Temperton, Francois Bouttier and Martin Miller are greatly appreciated.

## References

- Bruce, G H, D W Peaceman, H H Rachford Jr and J D Rice, 1953: *Trans Am Inst Min Metall Engnrs*, **198**, 79-92.
- Butler, S T and K A Small, 1963: The excitation of atmospheric oscillations, *Proc Roy Soc* **A274**, 91-121.
- Chapman, S and R S Lindzen, 1970: *Atmospheric tides*, Reidel, Dordrecht, Holland, 200 pp.
- Derber J. and F. Boutier, 1999: A reformulation of the background error covariance in the ECMWF global data assimilation system, *Tellus*, **51A**, 195-221.
- Hamilton, K, 1981: Latent heat release as a possible forcing mechanism for atmospheric tides, *Mon Wea Rev*, **109**, 3-17.
- Haurwitz, B, 1956: The geographical distribution of the solar semi-diurnal pressure oscillation, *Meteorol Pap*, **2**, (5), New York University.
- Hsu, H-H and B J Hoskins, 1989: Tidal fluctuations as seen in the ECMWF data. *Q J R Meteorol Soc*, **115**, 247-264.
- Lindzen, R.S., E.S. Batten and J.-W Kim, 1968: Oscillations in Atmospheres with Tops, *Mon Wea Rev*, **96**, 133-140.
- Jacchia, L G and Z Kopal, 1951: Atmospheric oscillations and the temperature profile of the upper atmosphere. *J Meteorol*, **9**, 13-23.
- Sen, H K and M L White, 1955: Thermal and gravitational excitation of atmospheric oscillations. *J Geophys Res*, **60**, 483-495.
- Siebert, M, 1954: Zur theorie der thermischen Erregung gezeitenartigen Schwingungen der Erdatmosphäre. *Naturwissenschaften*, **41**, 446.
- Siebert, M, 1961: Atmospheric tides, in *Advances in Geophysics*, Vol 7, Academic Press, New York, 105-182.
- Zwiers, F and K Hamilton, 1986: Simulation of solar tides in the Canadian Climate Centre general circulation model. *J Geophys Res*, **91**, 11877-11896.

1. Introduction

2. Model description

3. Results

4. Discussion

5. Conclusions

6. Acknowledgements

7. References

8. Appendix

9. Figures

10. Tables

11. Glossary

12. Index

13. Bibliography

14. List of symbols

15. List of abbreviations

16. List of acronyms

17. List of figures

18. List of tables

19. List of references

20. List of authors

21. List of contributors

22. List of reviewers

23. List of sponsors

24. List of funding agencies

25. List of funding numbers

26. List of funding dates

27. List of funding amounts

28. List of funding conditions

29. List of funding terms

30. List of funding conditions

31. List of funding terms

32. List of funding conditions

33. List of funding terms

34. List of funding conditions

35. List of funding terms

36. List of funding conditions

37. List of funding terms

38. List of funding conditions

39. List of funding terms

40. List of funding conditions

41. List of funding terms

42. List of funding conditions

43. List of funding terms

44. List of funding conditions

45. List of funding terms

46. List of funding conditions

47. List of funding terms

48. List of funding conditions

49. List of funding terms

50. List of funding conditions

51. List of funding terms

52. List of funding conditions

53. List of funding terms

54. List of funding conditions

55. List of funding terms

56. List of funding conditions

57. List of funding terms

58. List of funding conditions

59. List of funding terms

60. List of funding conditions

61. List of funding terms

62. List of funding conditions

63. List of funding terms

64. List of funding conditions

65. List of funding terms

66. List of funding conditions

67. List of funding terms

68. List of funding conditions

69. List of funding terms

70. List of funding conditions

71. List of funding terms

72. List of funding conditions

73. List of funding terms

74. List of funding conditions

75. List of funding terms

76. List of funding conditions

77. List of funding terms

78. List of funding conditions

79. List of funding terms

80. List of funding conditions

81. List of funding terms

82. List of funding conditions

83. List of funding terms

84. List of funding conditions

85. List of funding terms

86. List of funding conditions

87. List of funding terms

88. List of funding conditions

89. List of funding terms

90. List of funding conditions

91. List of funding terms

92. List of funding conditions

93. List of funding terms

94. List of funding conditions

95. List of funding terms

96. List of funding conditions

97. List of funding terms

98. List of funding conditions

99. List of funding terms

100. List of funding conditions

## Appendix

Here we would like to emphasise that the analysis of the  $S_1$  and  $S_2$  tides in the model atmosphere may provide a useful diagnostic of changes in an atmospheric analysis and forecast system. The tidal information is obtained in a straightforward way once the monthly mean files have been generated. We took the monthly means of the logarithm of the surface pressure because these are available for analysis, first-guess and forecast. The  $S_1$  tide is then obtained by the operation  $(12Z-00Z)/2$  while the  $S_2$  tide follows from  $(00Z+12Z-06Z-18Z)/4$  where the numbers refer to the times the monthly means are valid.

In order to illustrate the usefulness of this tool we have studied the introduction of the new formulation of  $J_B$  in the ECMWF variational scheme in May 1997 (Derber and Bouttier, 1999). Fig 10 shows the spatial distribution of the  $S_1$  tide from analysis, first-guess and the difference between first-guess and analysis for April 1997 while Fig 11 shows the corresponding plots for June 1997. Marked changes in the error pattern are to be noted when Fig 10c and 11c are compared, in particular over central Africa, Siberia, the southern Atlantic, South America and South Africa.

Marked changes are also noted in the error plots of the  $S_2$  tide shown in Figs 12 and 13 for April and June 1997. In this case it involves the southern ocean west of South America, South America, the Hudson Bay, Greenland and Europe.

It is too much in this context to try to find reasons for the discrepancies found. However, it should be mentioned that apart from the new formulation of the background error another change was introduced in May 1997. Before that time, surface pressure observations were not used in the analysis of the large scales, while after that time they were used. The work of Haurwitz (1956) has shown that long time series of pressure observations are needed in order to obtain a tidal signal out of the noise (caused by measurement errors and local features). It may therefore not be a good idea to buy the large scale information in the pressure observations. Although an analysis scheme is a useful instrument to extract coherent features out of a noisy signal, it requires that sufficient weight is given to the background. In the context of the tides this point has not been studied.

We concentrate for now on the biggest difference which is the one over central Africa in the  $S_1$  tide. First of all, we remark that this difference not only occurs in June 97 but is found in all successive months (and also after 4DVAR was introduced in November 1997). Typically, the first-guess amplitude is larger than the analysed one and the difference is more than one mb.

However, if one determines the  $S_1$  tide at 18Z by using the mean fields at 18Z and 06Z then it is quite remarkable to see that over central Africa there is hardly any difference between first-guess and analysis. In fact, analysed tide is now somewhat larger than first-guess tide.

This picture is confirmed by analysing time series of the difference between observations and first-guess surface pressure observations. Subtracting the mean difference of 00Z from the one at 12Z and dividing by 2 gives a measure of the difference between observed and first-guess tidal amplitude. We took the month of May 1999 and considered stations with a regular reporting practice in a small box around the equator in central Africa. For the 12Z tide we found an error of +0.65 mb, indeed indicating that the first-guess tide is too strong (note that tidal amplitudes are negative over central Africa) while for the 18Z tide we found an



error of -0.6 mb indicating that the first-guess tide is somewhat weaker than the analysed one. To be sure, it is not at all clear why the present analysis-forecasting system is behaving in such an odd way.

Nevertheless, when comparing the first-guess  $S_1$  tide at 12Z with the observational evidence presented in *Chapman and Lindzen (1970)* which gives amplitudes of the order of 0.9 mb, it seems that over central Africa the ECMWF model gives a too large diurnal tidal amplitude. Unfortunately, although the observations try to correct this defect, it seems that this information is rapidly lost in the forecast of the  $S_2$  tide.

We finally remark the following about the simulation of the  $S_2$  tide (cf Figs 12 and 13). First, it is believed that the modelled  $S_2$  tide has a too strong amplitude. Concentrating for the moment on the tropical Atlantic, one typically finds amplitudes between 1.4 and 1.75 mb whereas the empirical fit of Haurwitz suggests an amplitude of 1.16 mb. Regarding the phase of the  $S_2$  tide we note that before May 1997 analysed and forecast maximum amplitude was obtained at  $45^\circ$  W which corresponds to 9 o'clock local solar time. Although this is in fair agreement with simple tidal theory, it is not quite in agreement with the observational evidence of Haurwitz which suggests a maximum close to 10 o'clock corresponding to  $30^\circ$  W. However, to be fair, it should be pointed out that the maximum is not always well defined. In contrast, after May 1997 the analysis suggests a maximum at 10 o'clock local time while the first-guess still has its maximum at 9 o'clock.

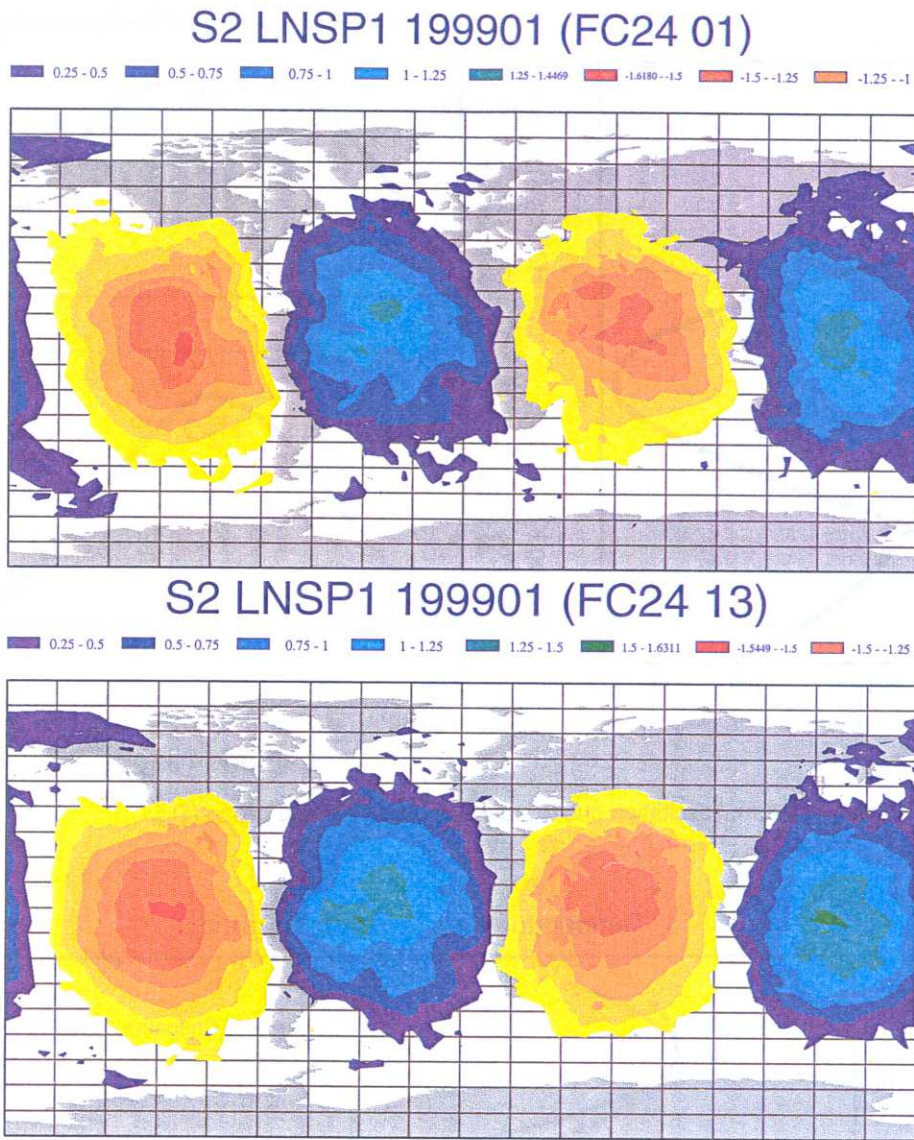


Fig. 1 Comparison of day 1 forecast S<sub>2</sub> tide of L31 version (top) and L50 version of the ECMWF model for January 1999.

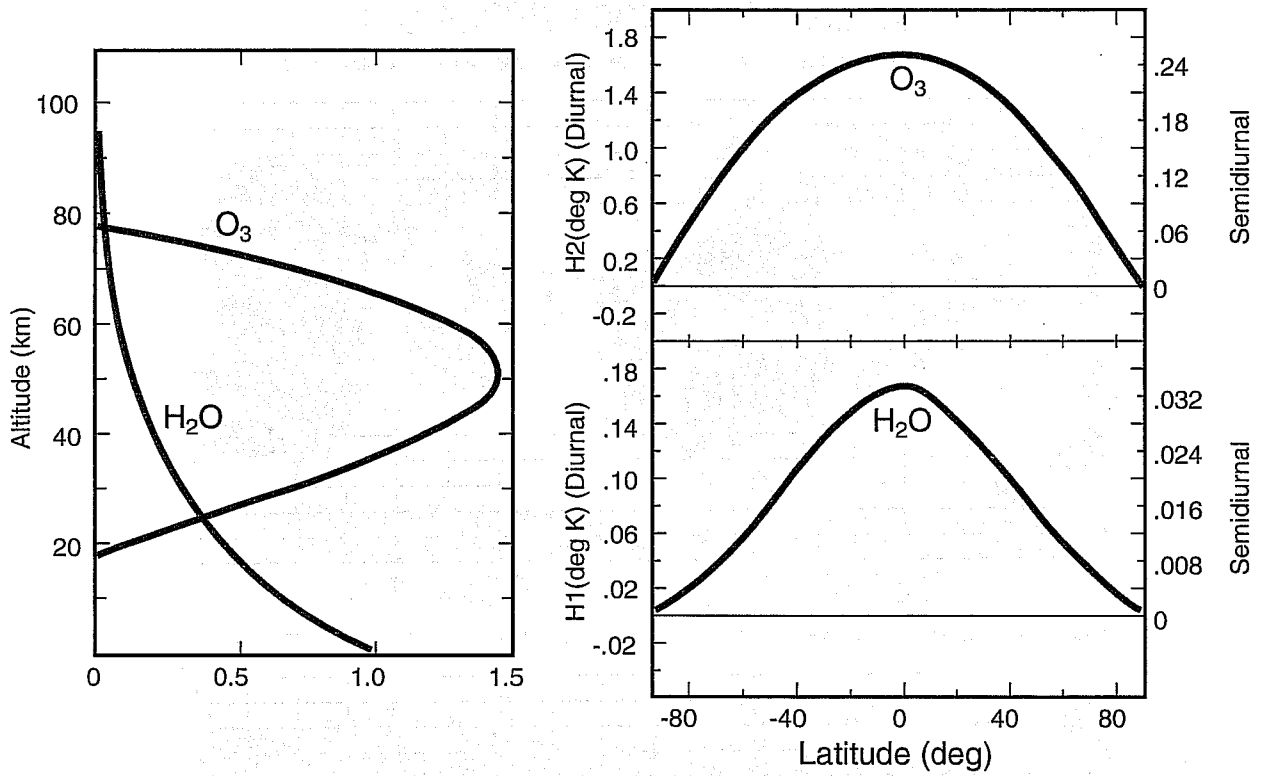


Fig. 2 Vertical distribution of thermal excitation due to water vapour ( $H_2O$ ) and ozone ( $O_3$ ).

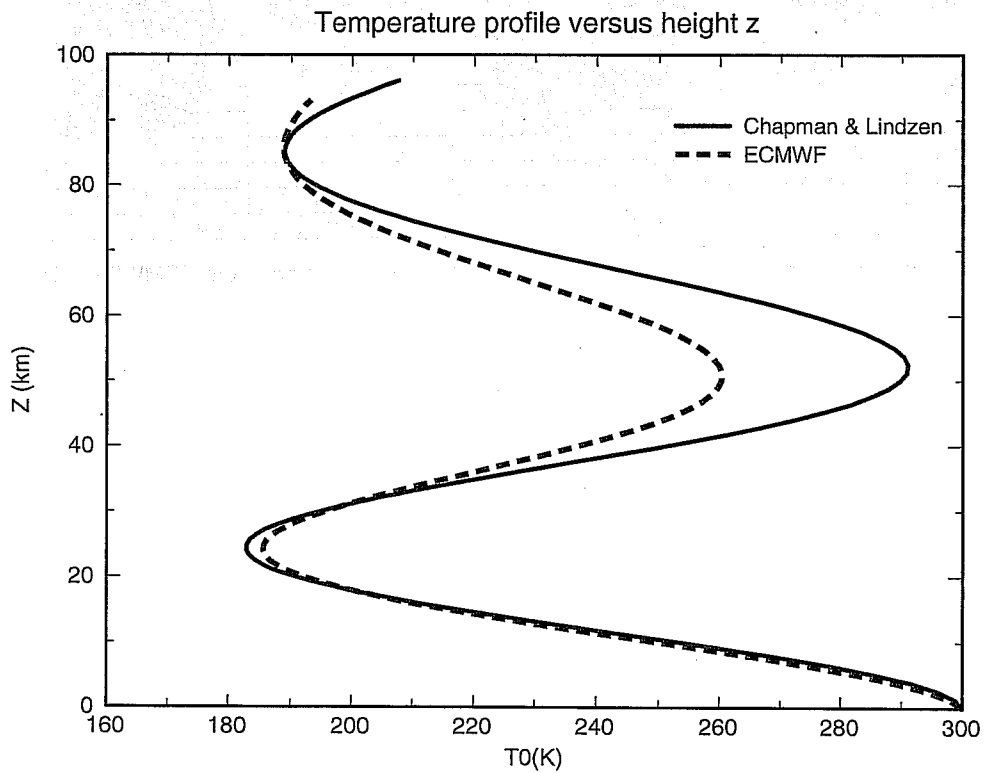


Fig. 3 Temperature profile as function of height.

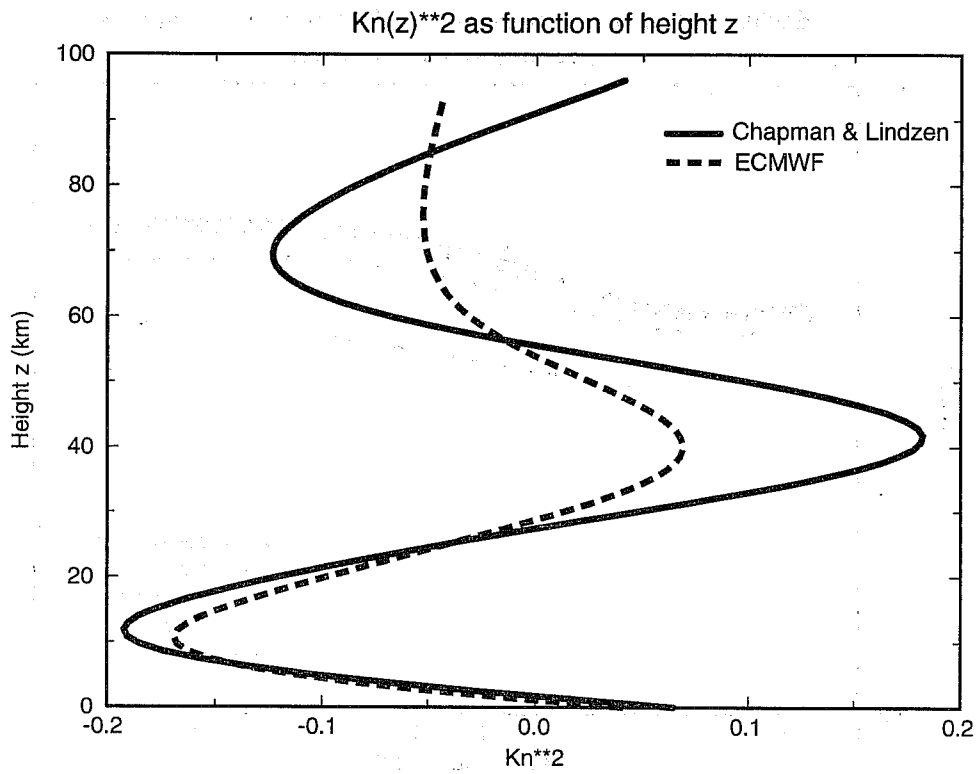


Fig. 4 The square of the vertical wave number for the temperature profiles of Fig. 3 versus height.

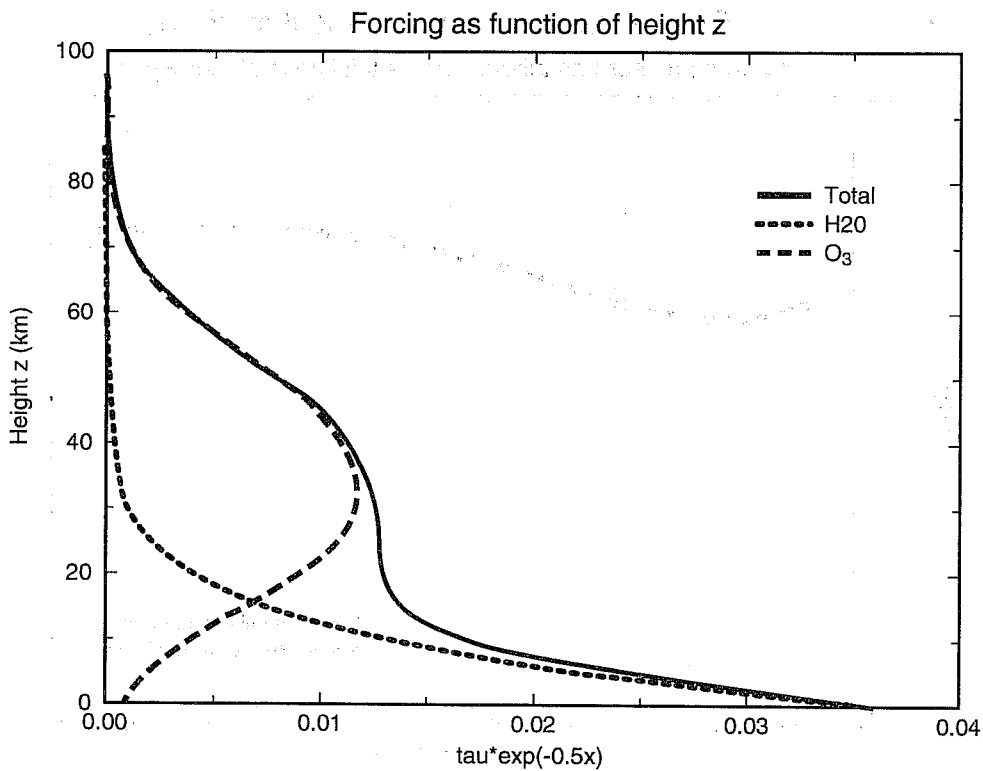


Fig. 5 Forcing by ozone and water vapour versus height.

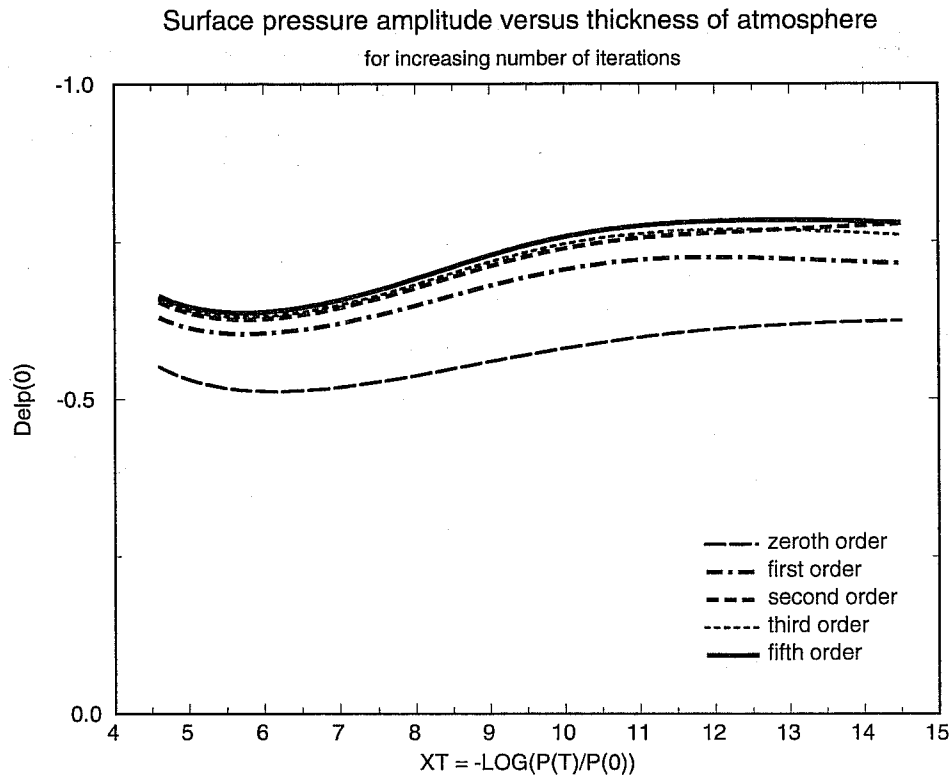


Fig. 6 Test of convergence of iteration scheme illustrated for the dependence of surface pressure amplitude on the thickness of the atmosphere.

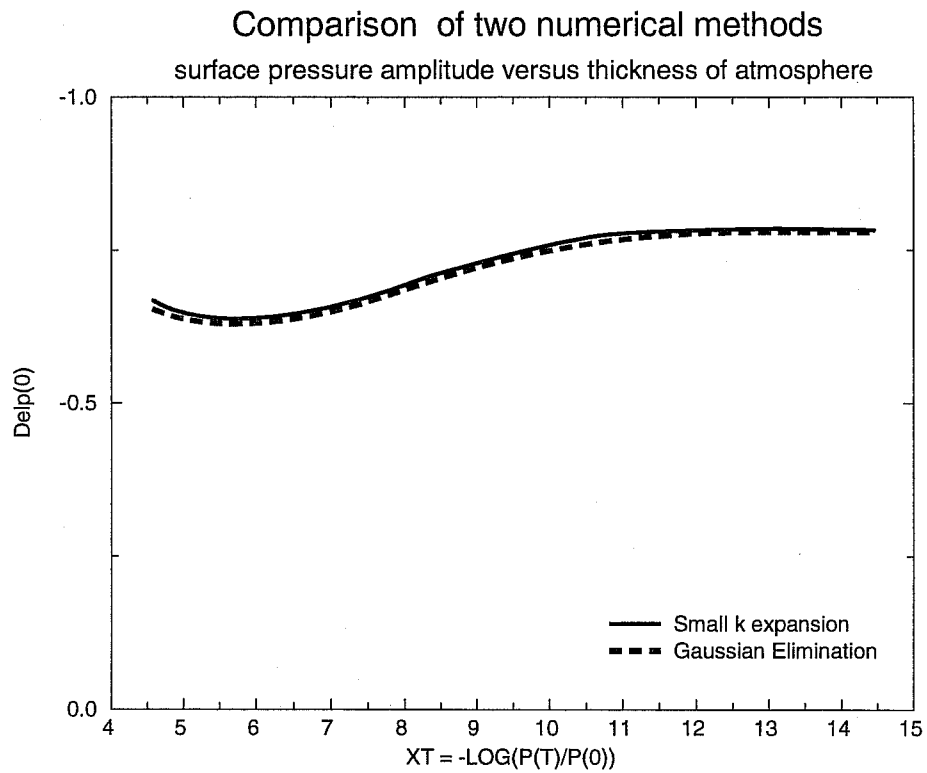


Fig. 7 Comparison of Gaussian elimination method with solution from iteration method.

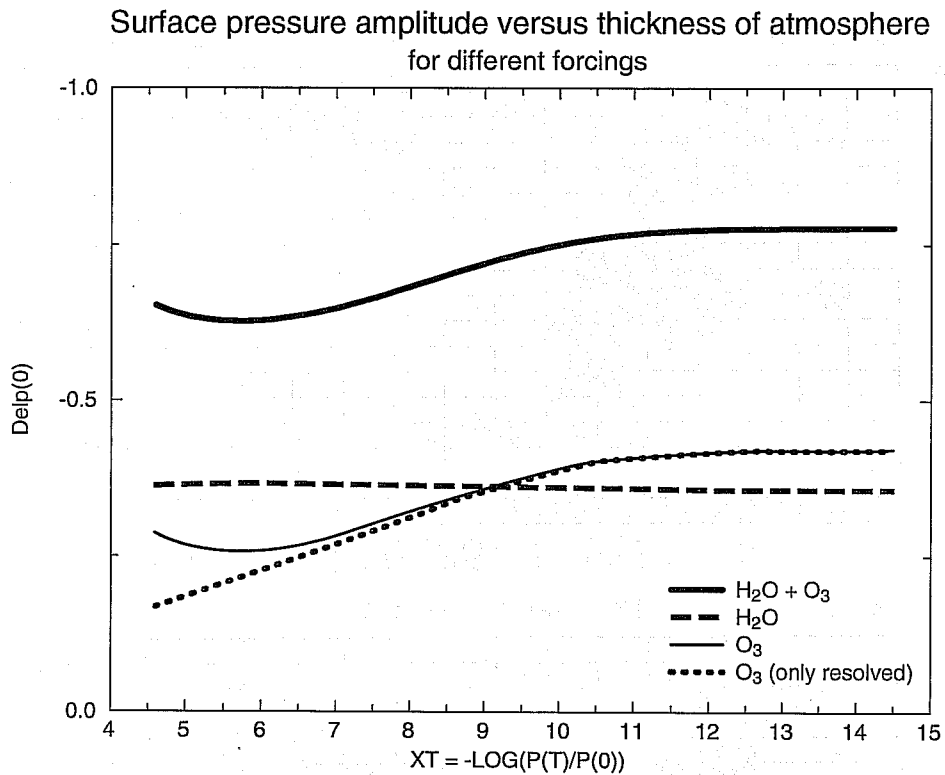


Fig. 8 Contributions of water vapour and ozone to the  $S_2$  surface pressure amplitude, using the 'ECMWF' mean temperature profile.

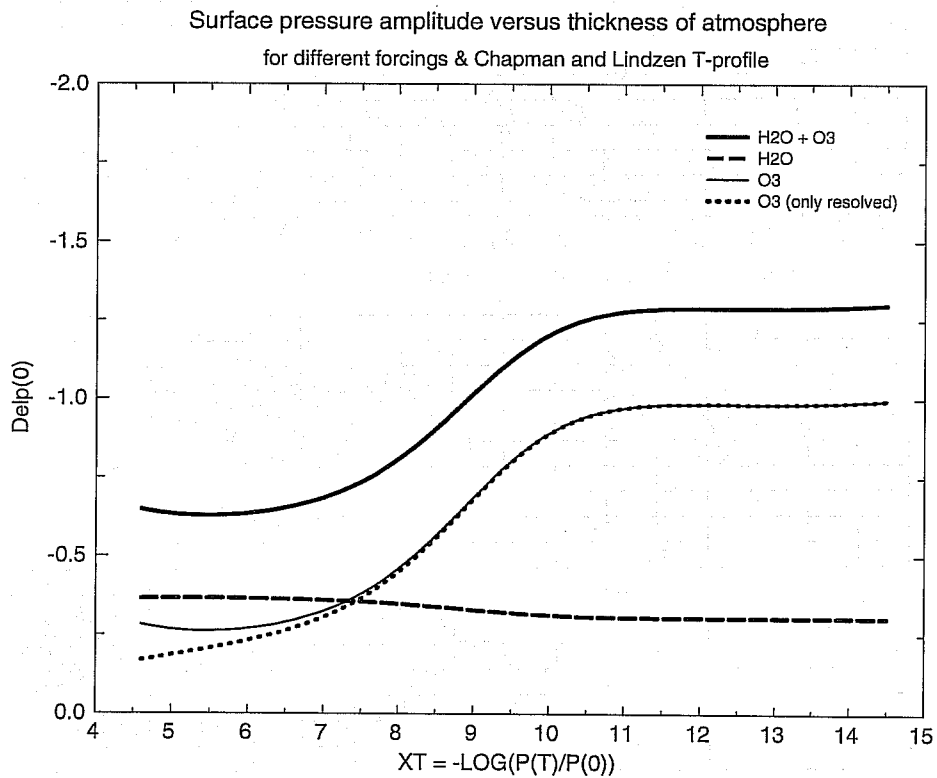


Fig. 9 Contributions of water vapour and ozone to the  $S_2$  surface pressure amplitude, using the equatorial temperature profile of Chapman and Lindzen. Now for large  $x_T$ , the ozone contribution dominates.

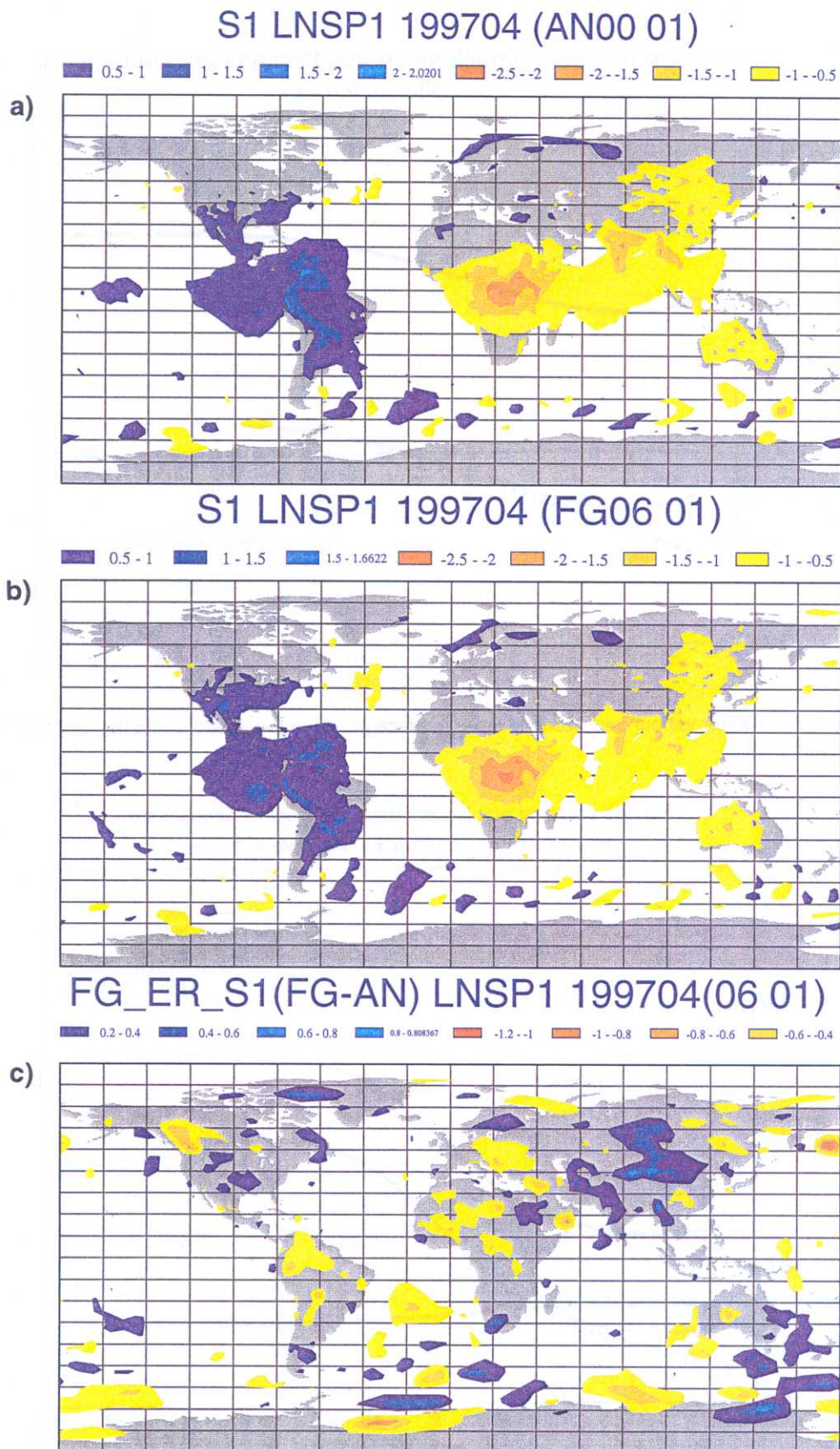


Fig. 10  $S_1$  tide according to a) analysis, b) first-guess and c) their difference for April 1997.

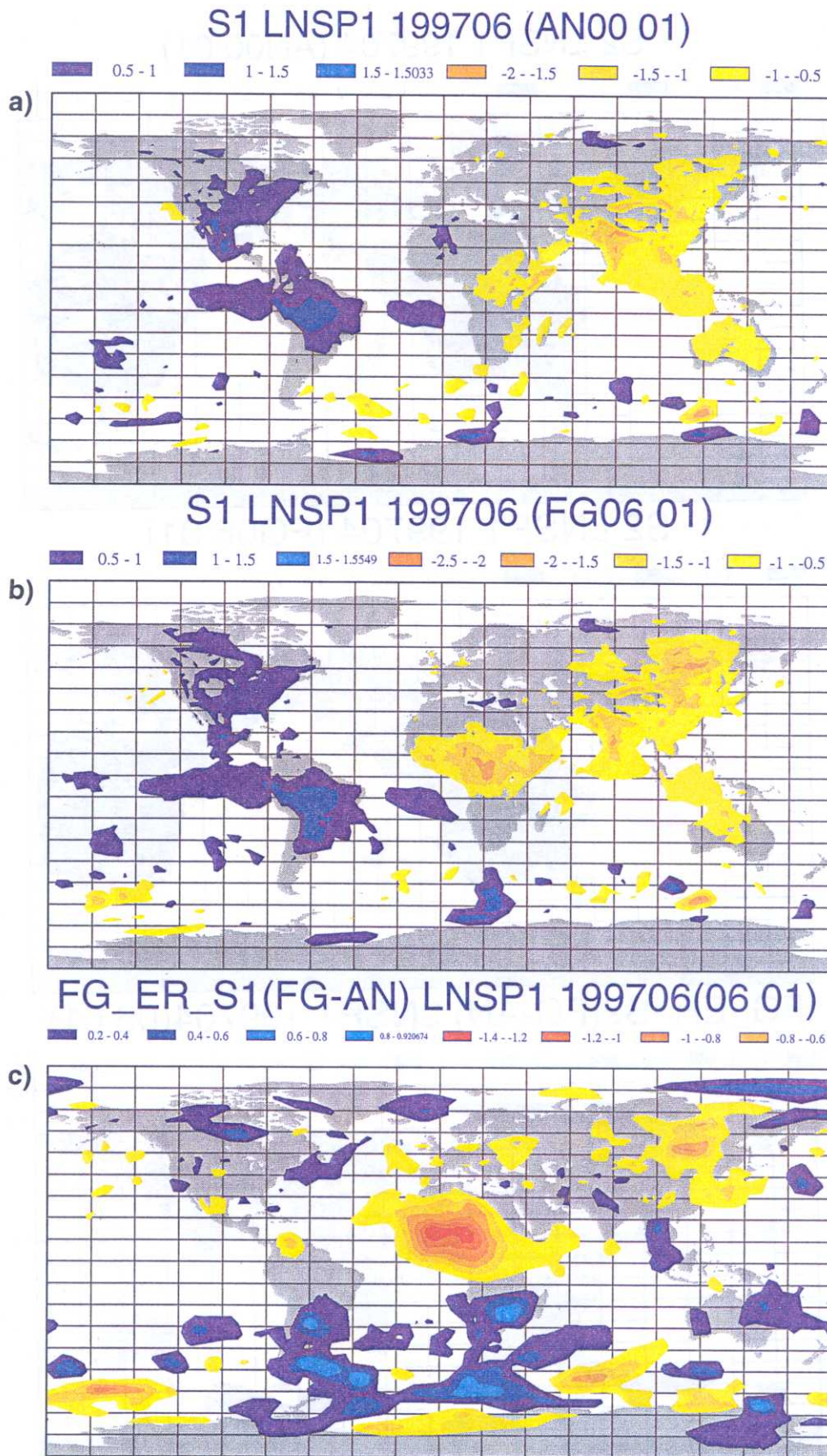


Fig. 11 Similar to Fig 10 but now for June 1997



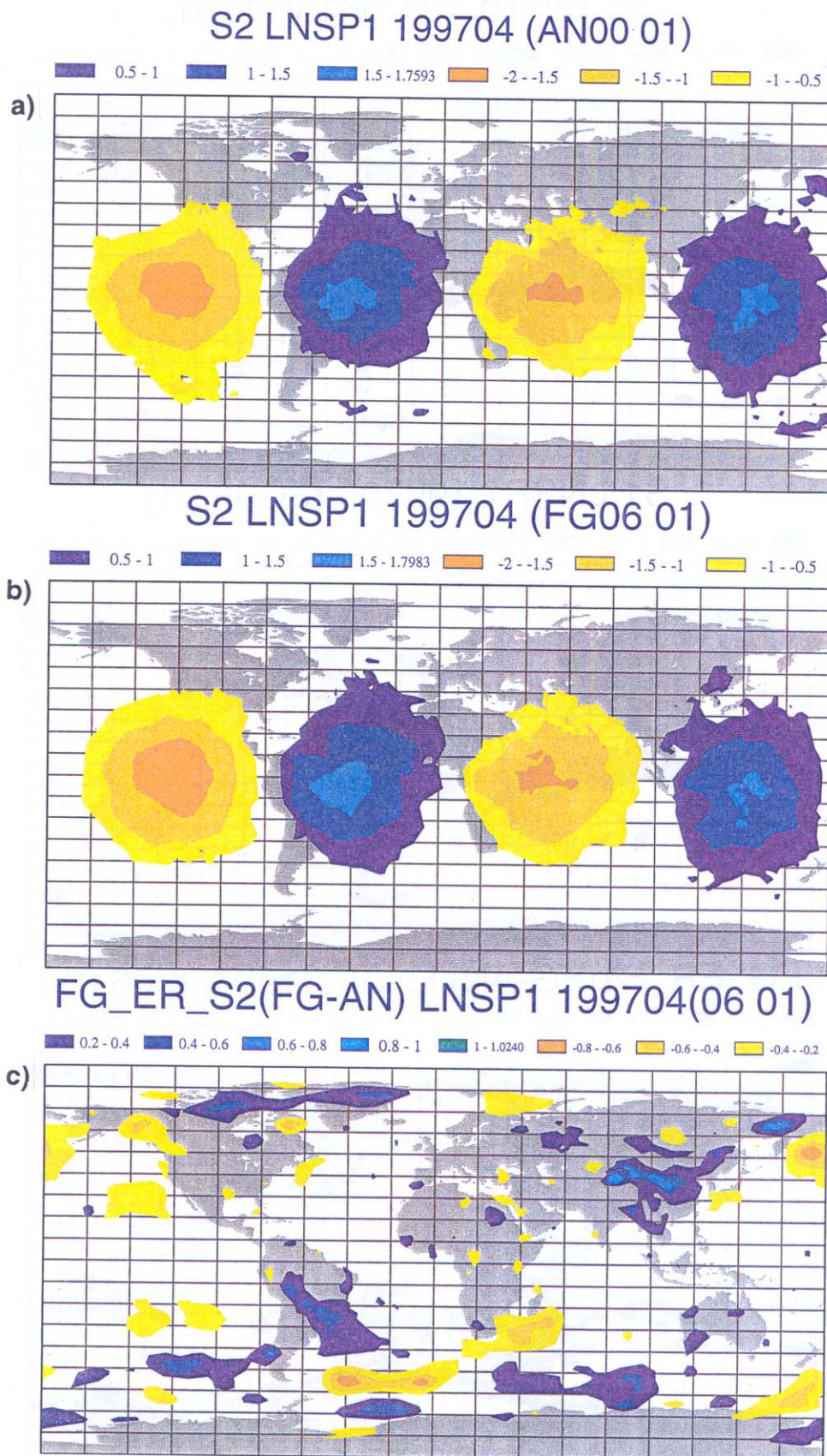


Fig. 12  $S_2$  tide according to a) analysis, b) first-guess and c) their difference for April 1997.

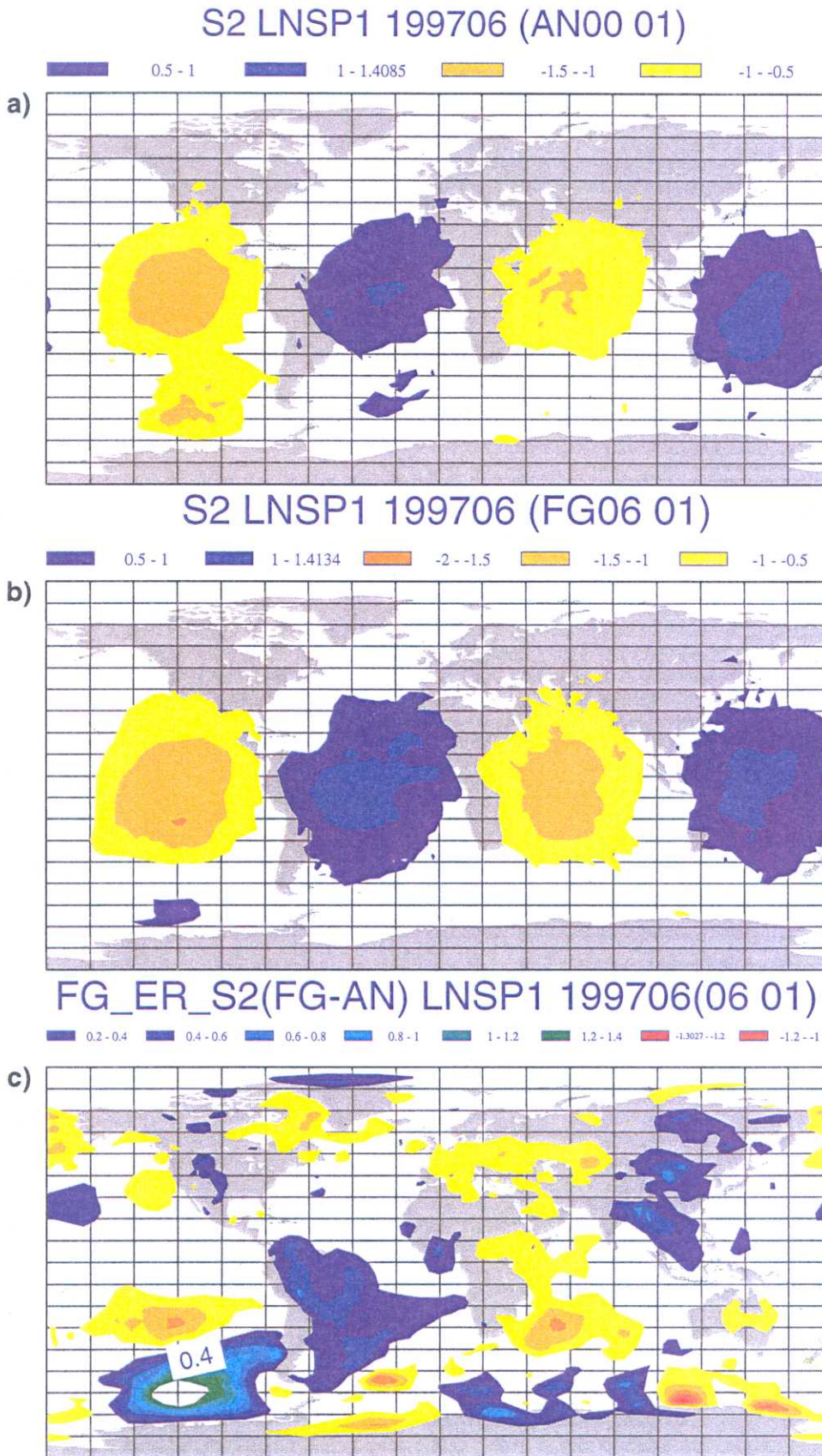


Fig. 13 Similar to Fig 12 but now for June 1997.